

TGF- β 1 modulates temozolomide resistance in glioblastoma via altered microRNA processing and elevated MGMT

Er Nie^{1#}, Xin Jin^{2#}, Faan Miao¹, Tianfu Yu³, Tongle Zhi⁴, Zhumei Shi⁵, Yingyi Wang⁵, Junxia Zhang^{5*}, Manyi Xie^{1*} and Yongping You^{5*}

¹Department of Neurosurgery, The Affiliated Hospital of Xuzhou Medical University, Xuzhou, Jiangsu Province, PR China.

²Department of medicine, Nanjing Gaochun People's Hospital, Nanjing, Jiangsu Province, PR China.

³Department of Neurosurgery, The Affiliated Drum Tower Hospital, School of Medicine, Nanjing University, Nanjing, Jiangsu Province, PR China.

⁴Department of Neurosurgery, Yancheng City No.1 People's Hospital, The Fourth Affiliated Hospital of Nantong University, Yancheng, Jiangsu Province, PR China.

⁵Department of Neurosurgery, the First Affiliated Hospital of Nanjing Medical University, Nanjing, Jiangsu Province, PR China.

#These authors contributed equally to the manuscript.

*Corresponding Authors: Junxia Zhang, M.D., Department of Neurosurgery, The First Affiliated Hospital of Nanjing Medical University, 300 Guangzhou Road, Nanjing 210029, Jiangsu Province, China (zjx2032@126.com); Manyi Xie, MD, Department of Neurosurgery, The Affiliated Hospital of Xuzhou Medical University, 99 Huaihai West Road, Xuzhou 221000, Jiangsu Province, China (aman_80@126.com) and Yongping You, MD, Department of Neurosurgery, The First Affiliated Hospital of Nanjing Medical University, 300 Guangzhou Road, Nanjing 210029, Jiangsu Province, China (yypl9@njmu.edu.cn)

Supplementary Materials and Methods

Patients and samples

A total of 46 patients (31 males and 15 females) with a median age of 47.5 years (range, 19–72 years) who had been treated surgically at the Department of Neurosurgery, The First Affiliated Hospital of Nanjing Medical University (Nanjing, China), between January 2013 and October 2015 were selected for the study. Among the 46 cases, 41 tumor samples and five non-tumorous brain specimens were obtained for analysis from the patients registered at the hospital. This study was approved by the institutional review board and the Research Ethics Committee of Nanjing Medical University (Nanjing, Jiangsu, China). Informed consents were obtained from all participants. All methods were performed in accordance with the approved guidelines.

The gliomas tissue samples were histologically diagnosed by the Department of Pathology at The First Affiliated Hospital of Nanjing Medical University according to the WHO classification¹. As controls, five human non-tumor brain tissues (NBTs) samples were obtained primarily from the cortex of patients with decompressive surgery after physical injury to the brain. Samples were immediately snap-frozen in liquid nitrogen until use.

The TCGA database of glioma was downloaded from <http://tcga-data.nci.nih.gov>. The CGGA (the Chinese Glioma Genome Atlas) database^{2,3} was downloaded from <http://www.cgca.org.cn/>.

Cell culture and reagents

The human glioblastoma multiforme (GBM) cell lines A172, U87, U251, LN229, U138 and T98 were purchased from Shanghai Cell Bank of the Chinese Academy of Sciences (Shanghai, China). DBTRG-05MG (05MG) and D54 cell line was bought from Sigma-

Aldrich (St. Louis, MO, USA). Normal human astrocytes (NHAs) were obtained from Lonza (Walkersville, MD, USA) and cultured in the provided astrocyte growth media supplemented with rhEGF, insulin, ascorbic acid, GA-1000, L-glutamine and 5% FBS. The primary GBM1 and primary GBM2 cell lines were established as described previously⁴. TMZ resistant cells-P-GBM2-R cells were generated by repetitive pulse exposure of P-GBM2 glioma cells to TMZ⁵. All GBM cell lines were validated in October 2015 by short tandem repeat DNA fingerprinting using the AmpFISTR Identifiler kit according to the manufacturer's instructions (Applied Biosystems, CA, USA). All GBM cell lines were preserved in liquid nitrogen to maintain authenticity. The cells used for the experiments were replenished from frozen stocks every 3 months. Cells were cultured in 5% CO₂ at 37 °C in Dulbecco's modified Eagle's medium (DMEM, Gibco, CA, USA) supplemented with 10% fetal bovine serum (Gibco).

Plasmids construction, transfection and stable cell establishment

Plasmids expressing has-TGF- β 1, has-lncRNA-H19, has-lncRNA-H19-mut, has-lncRNA-HOXD-AS2, Flag-KSRP-wt, or Flag-KSRP-mut(KH1,KH2,KH3,KH4) were provided by Genechem (Shanghai, China). KSRP-specific siRNAs (siKSRP: 5'-AAGATCAACCGAGAGCAAGA-3'), H19-specific siRNAs (siH19: 5'-CCC ACA ACAUGAAAGAACTT-3'), HOXD-AS2-specific siRNAs (siHOXD-AS2: 5'-CCCAAGGAUUCAGCAAACATT-3'), TGF- β 1-specific siRNAs (siTGF- β 1: 5'-GGACTACTACGCCAAAGAA-3') and nonspecific siRNA (NC: 5'-UUCUCCGAACGUGUCACGUTT-3') were purchased from GenePharma (Shanghai, China). Anti-Smad2/3 small interfering RNA (siRNA) (sc-37238), and control siRNA (sc-36869) were purchased from Santa Cruz (USA). Cells were transfected with plasmids or siRNAs using Lipofectamine™ 3000(Invitrogen) according to standard

protocols. For cells with stably expressing HOXD-AS2, H19 or TGF- β 1, GBM cells transfected with lentiviral particles for 48 hours were drug-selected using 5 μ g/ml puromycin for 4 weeks in selection media. Puromycin-resistant colonies were selected and screened for molecules expression. The pCDNA3.1(-)-12xMS2 vector was excised from the pCDNA3.1(-)-SLNCR1-12xMS2 (Addgene, 86828). Full-length H19 were PCR-amplified from human cDNA and subcloned into pCDNA3.1(-)-12xMS2 to create pCDNA3.1(-)-H19-12xMS2 expression plasmids. All plasmids were sequenced before their use.

Immunofluorescence staining

Cells grown on confocal dishes (Cellvis, CA, USA) were fixed for 30 min in 4% paraformaldehyde at room temperature, and then incubated in PBS containing 0.1% Triton X-100 for 15 min, and incubated with 1% BSA for 2h before incubation with anti-KSRP antibody overnight at 4 °C. Cells were washed 3 times in PBS for 5 min each, and then incubated with Alexa Fluor® 488 donkey anti-Rabbit IgG (H+L) (Jackson, PA, USA) secondary antibodies at room temperature for 2h. After a final wash with PBS, cells were incubated with 4, 6-diamidino-2-phenylindole (DAPI, CST, MA, USA) for 15min. The dishes were washed three times in ice-cold PBS. Images were captured with a Zeiss LSM 510 Meta confocal microscope (Zeiss, Oberkochen, Germany).

Co-immunoprecipitation (Co-IP)

Cells were lysed in SDS lysis buffer on ice for 30 min, and the supernatants were collected by centrifugation at 4°C and 14,000 \times g for 15min. The cleared protein lysates were then incubated with primary antibodies with rotation overnight at 4°C. Then, the

mixtures were incubated with immobilized protein G beads (Cell Signaling Technology) with rotation at 4°C for 2h. The beads were collected by centrifugation at 3,000×g for 2min, and then washed five times with 0.5ml IP wash buffer. SDS loading buffer was added to the beads, and the samples were denatured at 95°C for 8–10min. Finally, the supernatants were collected and stored at –80°C or immediately analyzed by WB.

Chromatin immunoprecipitation

Chromatin immunoprecipitation (ChIP) assays were performed using the EZ-magna ChIP kit (Millipore, Bedford, MA, USA) according to the manufacturer's protocol. The chromatin solution was immunoprecipitated overnight at 4°C with 50µl of protein A/G magnetic beads (Millipore) and 5µg of indicated antibody. Control samples were immunoprecipitated with 5µg IgG (Cell Signaling Technology, Danvers, MA, USA). After immunoprecipitation, the beads were washed sequentially with low-salt buffer; high-salt buffer, LiCl buffer, and TE buffer each for 5min at 4°C. The immunoprecipitated DNA was then eluted by incubation in 100µl of elution buffer (0.1M NaHCO₃ and 1% SDS) containing 10µg proteinase K (Sigma-Aldrich) at 62°C for 2h with rotation. The eluted DNA was purified using the columns and buffers contained in the kit (Millipore), and was finally re-dissolved in 50µl of PCR-grade water. The eluted DNA was subjected to quantitative PCR using SYBR Green master mix (Roche Applied Science, Upper Bavaria, Germany).

Orthotopic xenograft study

All experiments involving mice were approved by The Model Animal Research Center of Nanjing University (Nanjing, China). The mice were randomly divided into 10 mice per group. For orthotopic xenograft studies, GBM cells (2.5×10^5) with the indicated

125 treatment were injected intracranially into the striatum of NOD/SCID mice using a
126 stereotactic device (coordinates: 2 mm anterior, 2 mm lateral, 3 mm depth from the
127 dura). At the 7th day, the tumor-bearing mice were given TMZ by oral gavage (66
128 mg/kg daily for 5 days) for 3 cycles. Mice were sacrificed upon signs of tumor
129 formation (rough coat, hunching, and weight loss). Tumors were measured by
130 luminescence imaging (IVIS Spectrum, PerkinElmer, USA) each week. All animal
131 experiments were conducted with the approval of the Nanjing Medical University
132 Institutional Committee for Animal Research and in conformity with national
133 guidelines for the care and use of laboratory animals.

134 **Supplementary Table1**135 **List of antibodies used for western blot, CHIP or RIP**

antibody	Description
FSTL1	Thermo Fisher Scientific
FLAG	Sigma-Aldrich
β -actin	Cell Signaling Technology
KSRP	Cell Signaling Technology
Dicer	Cell Signaling Technology
Drosha	Cell Signaling Technology
MGMT	Cell Signaling Technology
Caspase-3 and cleaved caspase-3	Cell Signaling Technology (#9665)
γ -H2AX	Cell Signaling Technology
H2AX	Cell Signaling Technology
GAPDH	Cell Signaling Technology
Anti-Histone H3 (tri methyl K27)	Abcam

136

137 **Supplementary Table 2**138 **List of primers used for qRT-PCR, RIP or CHIP**

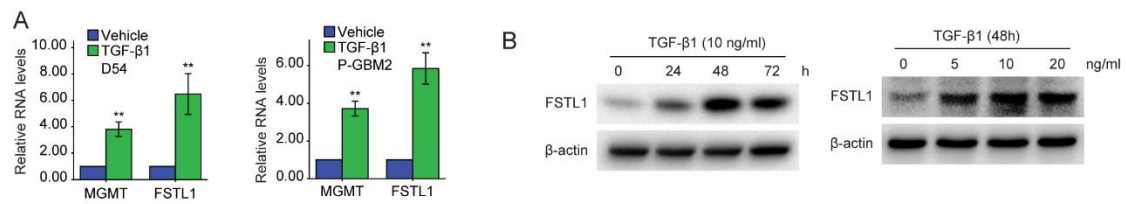
	Forward primer	Reverse primer	Remarks
pre-FSTL1	gggatctctgggaatggaata	acactgataggccacaaatgc	Binds within Intron 10
FSTL1	aatccaagatctgtgccaatg	gctgtacagaccaattcca	qRT-PCR

			Primers
KSRP	ctgttttgtttggcgagagag	gagacacagaacaggcgagag	qRT-PCR Primers
FSTL1	gagttggccctgtctcttctt	cttcccactctcttctctgct	RIP Primers
H19	actcaggaatcggctctggaa	ctgctgttccgatggtgtctt	qRT-PCR Primers
H19	gcaccttggacatctggagt	ttcttccagccctagctca	RIP Primers
HOXD-AS2	gacaaaggaactgctctgggtg	cttcttgtgtcctctgcttcc	qRT-PCR Primers
HOXD-AS2	ctggtgaactccccctgaaa	cgtgtttgctgaatccttggg	RIP Primers
miR-181a	tgtagtcttttgaatggcata	gtttatgccatttcaaaagact	CHIP Primers

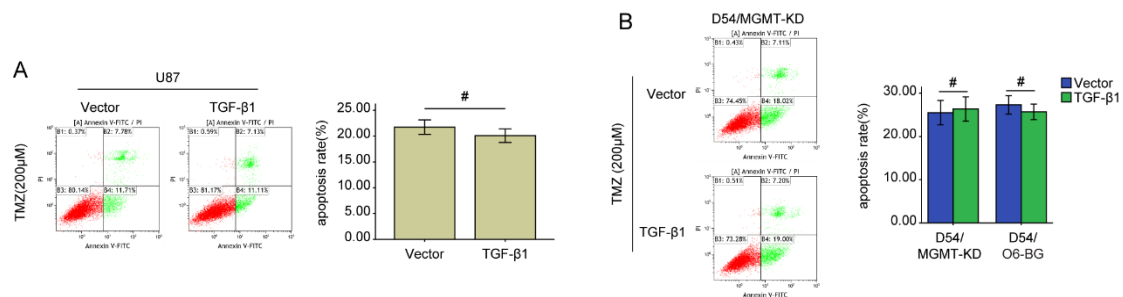
139

140

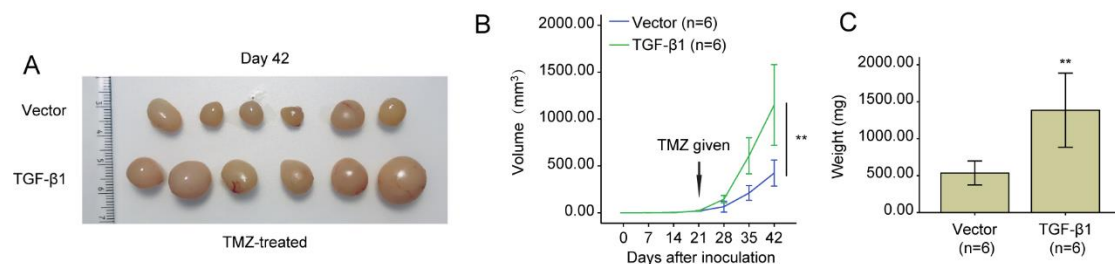
Supplementary Figures



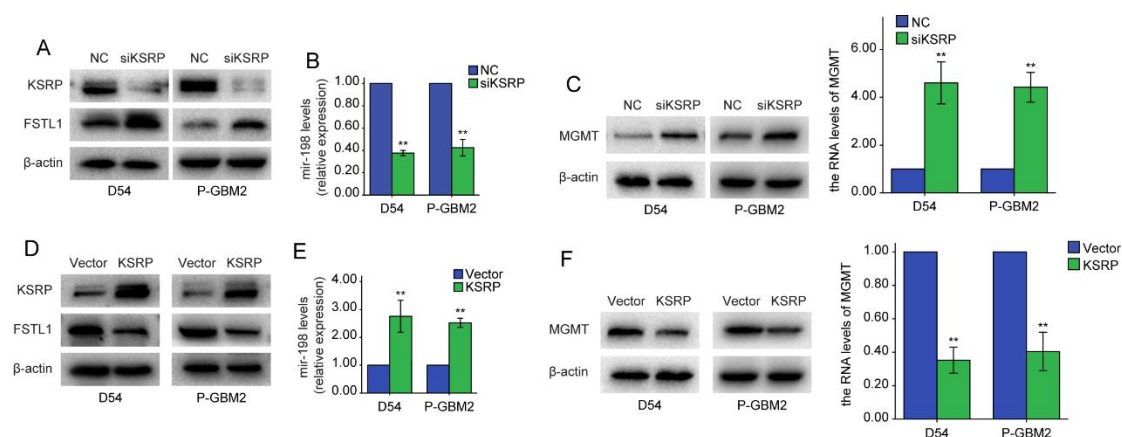
Supplementary Figure 1. A. GBM cells were incubated with vehicle or TGF-β1 (10 ng/ml) for 48h. The RNA levels of FSTL1 and MGMT were examined by qRT-PCR. B. The expression of FSTL1 was evaluated in D54 cells with TGF-β1 treatments using WB. Student's t-tests were performed. Data are presented as mean ± SEM (**P<0.01).



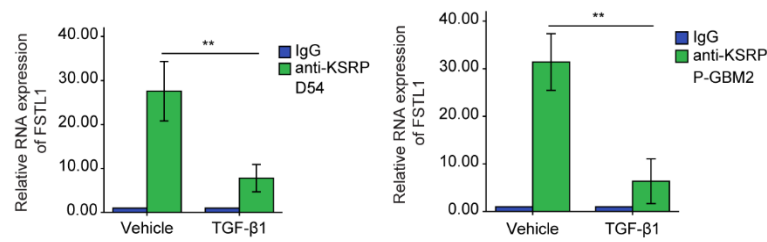
Supplementary Figure 2. TGF-β1 confers TMZ resistance through MGMT. A. U87 cells transfected with vector or TGF-β1 were treated with TMZ (200 μM) for 48 hours. Flowcytometry were used to measured cells apoptosis. B. MGMT expression was blocked using a lentivirus-mediated RNA interference (shMGMT) or MGMT inhibitor O6-benzylguanine (O6-BG, 20μM) in D54 cells stably expressing TGF-β1 plasmid or vector control. The cells were subsequently treated with TMZ (200 μM) for 48 hours. Flowcytometry was used to measured cells apoptosis. Student's t-tests were performed. Data are presented as mean ± SEM (#P>0.05).



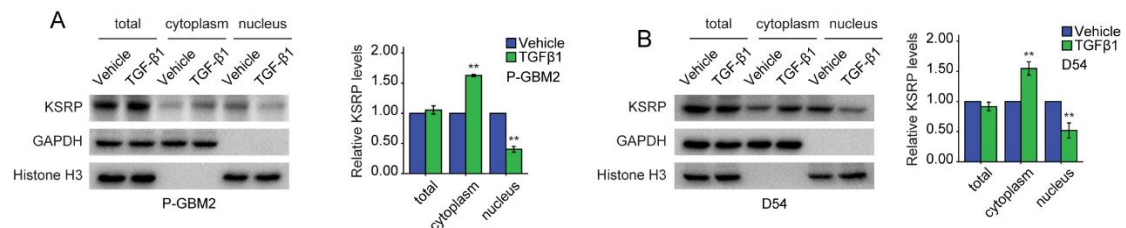
Supplementary Figure 3. TGF-β1 overexpression confers TMZ resistance *in vivo*. A, representative images of tumors originated from D54 cells stably expressing TGF-β1 or vector control in the presence of TMZ (66 mg/kg/day by oral gavage) on the 42nd day. B, growth curve of subcutaneous tumor xenografts. C, tumor weight is means of three independent experiments \pm SEM. Student's t-tests were performed. Data are presented as mean \pm SEM (**P<0.01).



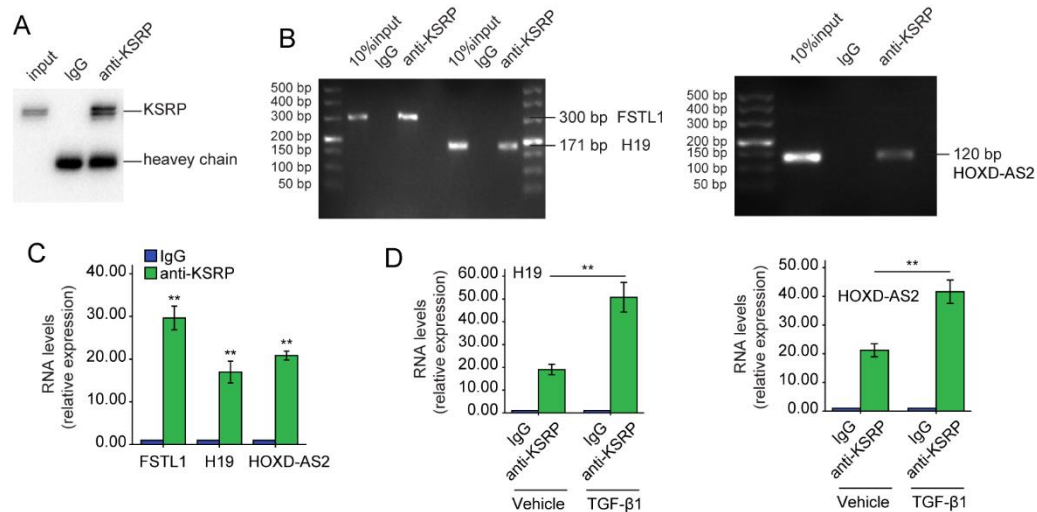
Supplementary Figure 4. Up or down KSRP influences FSTL1, MGMT and miR-198 expression. A-C, D54 and P-GBM2 cells transfected with negative control (NC) or siKSRP for 48h. QRT-PCR analysis for miR-198 and MGMT, Western blot analysis for KSRP, FSTL1 and MGMT. D-F, D54 and P-GBM2 cells transfected with vector or KSRP plasmid for 48h. QRT-PCR analysis for miR-198 and MGMT, Western blot analysis for KSRP, FSTL1 and MGMT. Results are representative of three independent experiments. Student's t-tests were performed. Data are presented as mean \pm SEM (**P<0.01).



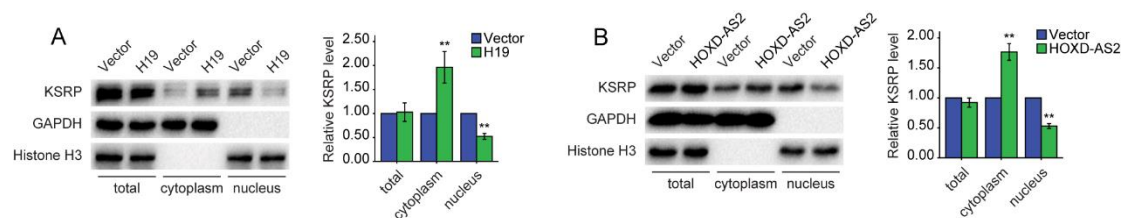
Supplementary Figure 5. GBM cells separately treated with or without TGF-β1 (10 ng/ml) for 48h. RIP was performed using anti-IgG or anti-KSRP antibody, and QRT-PCR analysis of FSTL1 expression. One-way ANOVA were performed. Data are presented as mean ± SEM (**P<0.01)



Supplementary Figure 6. TGF-β1 treatment influences KSRP distribution. The protein levels of KSRP in the cytoplasm and nucleus of GBM cells treated with or without TGF-β1 (10 ng/ml, 48h) were detected by WB. GAPDH and Histone H3 were used as loading control for cytoplasm and nucleus protein, respectively. Results are representative of three independent experiments. Student's t-tests. Data are presented as mean ± SEM (**P<0.01)

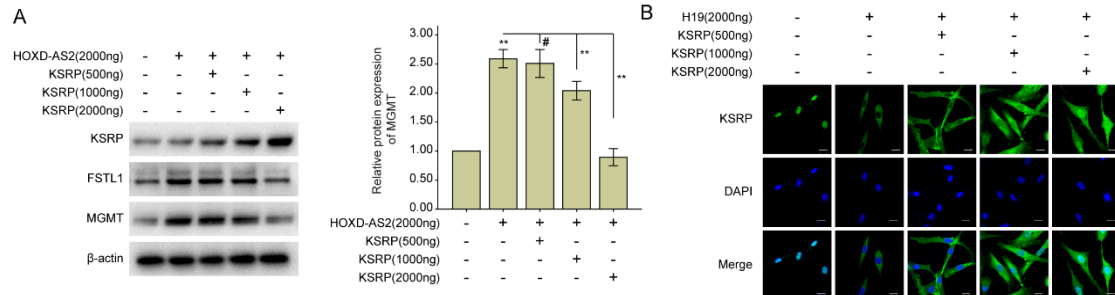


Supplementary Figure 7. TGF-β1 treatment promotes the binding of KSRP to H19 and HOXD-AS2. A, D54 cells were subjected to Co-IP analysis using anti-KSRP antibody for IP and blotting. B and C, RIP assays were performed using anti-IgG or anti-KSRP antibody. qRT-PCR showing fold enrichment of FSTL1, H19 and HOXD-AS2. D, D54 cells separately treated with or without TGF-β1 (10 ng/ml) for 48h. Total cell extracts were subjected to RIP assays using anti-IgG or anti-KSRP antibody, and RNA was purified from immunocomplexes and analyzed by RT-qPCR to detect H19 and HOXD-AS2. Student's t-tests were performed. Data are presented as mean ± SEM (**P<0.01),

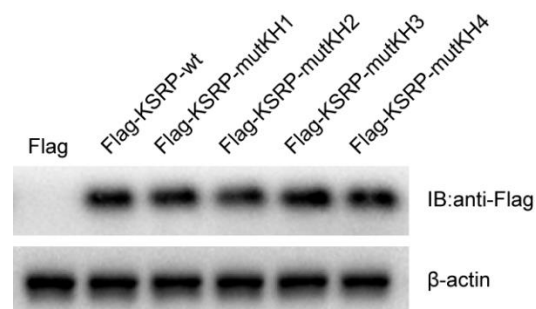


Supplementary Figure 8. H19 and HOXD-AS2 block the nuclear translocation of KSRP. The protein level of KSRP in the cytoplasm and nucleus after H19 or HOXD-AS2 overexpression in D54 cells for 48h. GAPDH and Histone H3 were used as loading control for cytoplasm and nucleus protein, respectively. Results are representative of

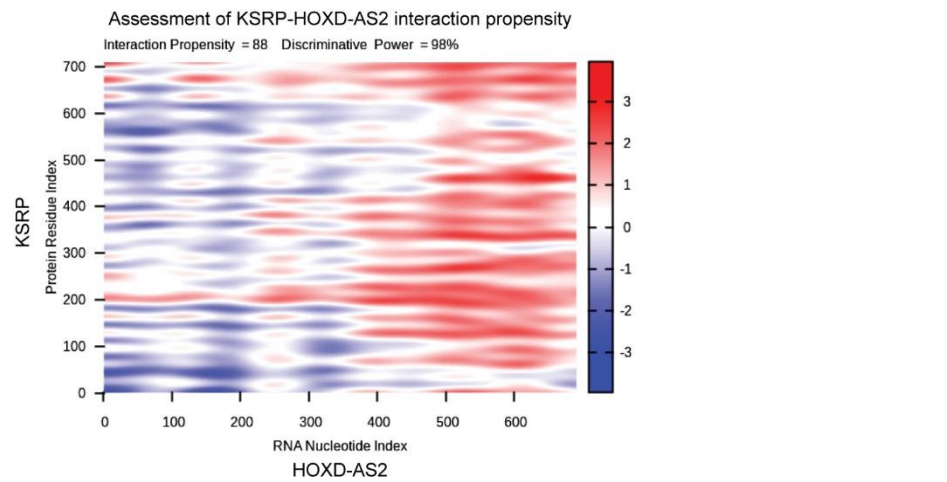
three independent experiments. Student's t-tests. Data are presented as mean \pm SEM (**P<0.01)



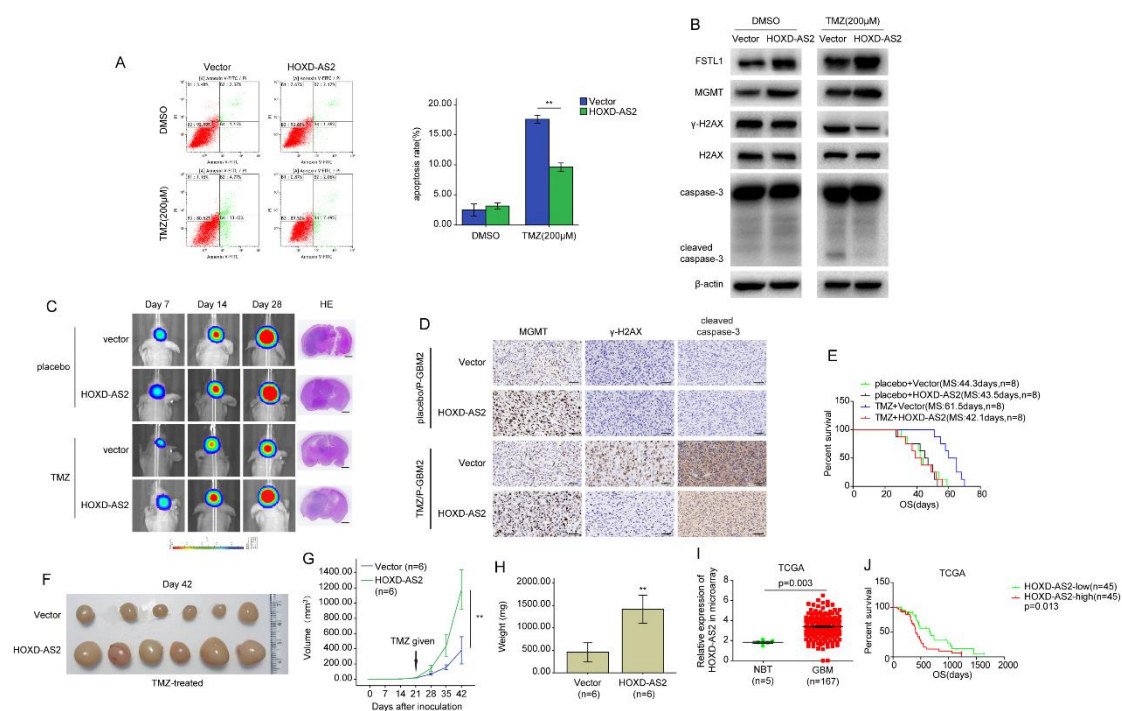
Supplementary Figure 9. Overexpression of KSRP reversed the effect of HOXD-AS2 on FSTL1. A, HOXD-AS2 and KSRP plasmids were co-transfected into D54 cells with indicated dosage. And WB analysis was performed using indicated antibodies. B, Immunofluorescence assay was performed on D54 cells co-transfected with HOXD-AS2(2000ng) or KSRP with indicated dosage, using anti-KSRP antibody (green). Merge: Green+Blue. Scale bar: 20 μ m. Results are representative of three independent experiments. One-way ANOVA were performed. Data are presented as mean \pm SEM (**P<0.01, #P> 0.05)



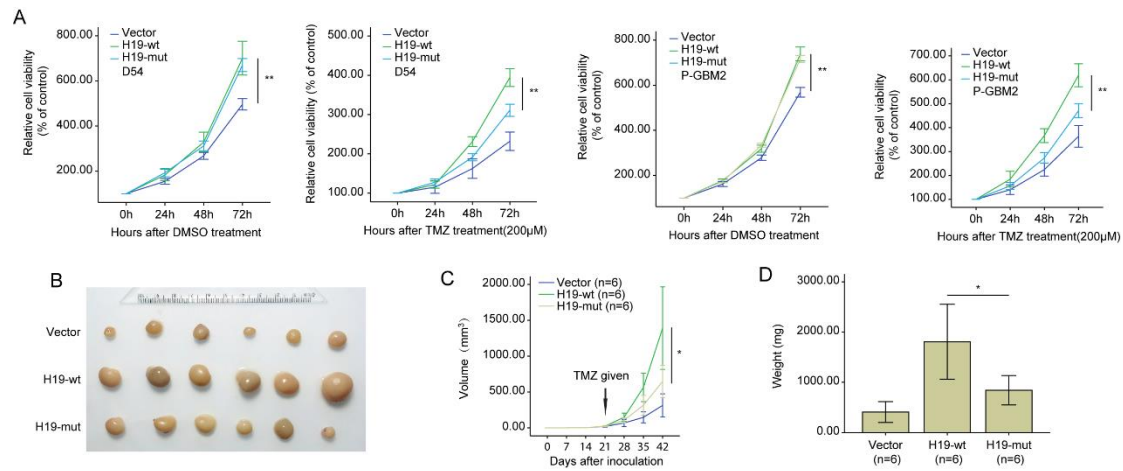
Supplementary Figure 10. Western blot analysis of the level of KSRP in D54 cells transfected with Flag, Flag-KSRP-wt or Flag-KSRP-mut using anti-Flag antibody.



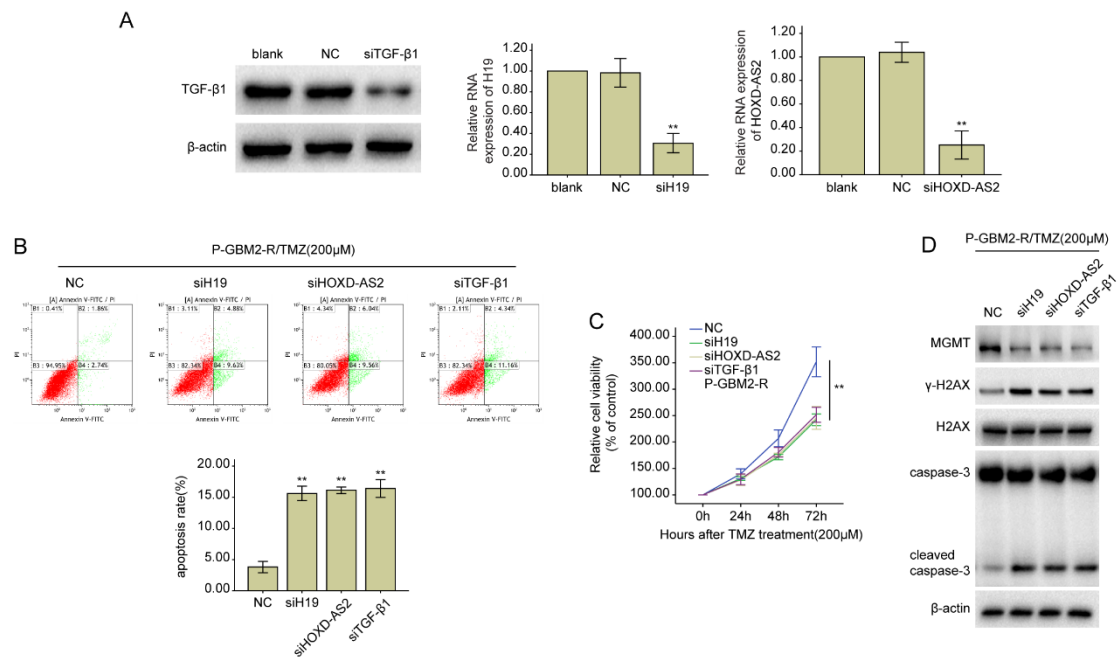
Supplementary Figure 11. In silico prediction of lncRNA-protein interactions supporting the proposed mechanism of lncRNAs functioning as a modular scaffold for chromatin modifiers and transcription factors. We used catRAPID graphics program⁶ to predict probability of protein-lncRNA interaction. Using HOXD-AS2 as an example, we tested the ability of the lncRNA to interact with KSRP shows that HOXD-AS2 and KSRP have an interaction propensity of 88%.



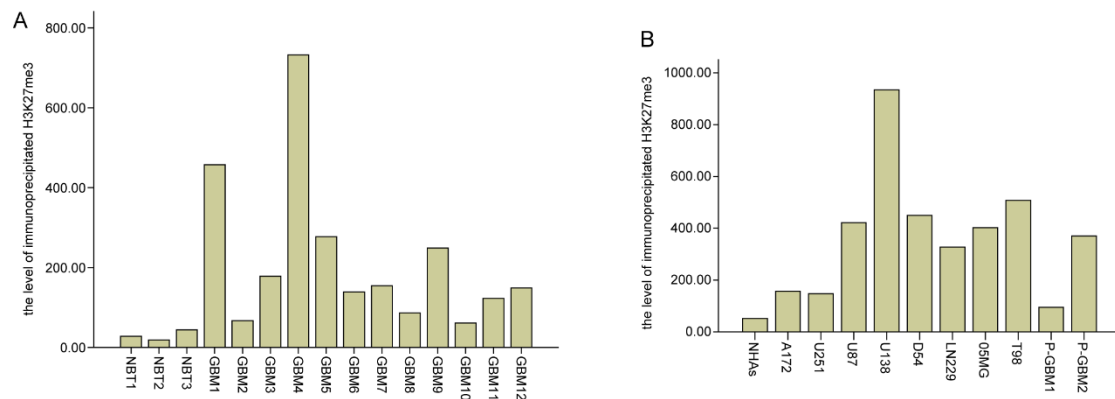
Supplementary Figure 12. HOXD-AS2 increases drug-resistance of GBM cells to TMZ. A and B, D54 cells infected with lentivirus expressing HOXD-AS2 or vector control were exposed to DMSO or 200 μ M TMZ for 48 hours. Flowcytometry were used to measured cells apoptosis, Western blot analysis for the indicated proteins. C, representative pseudocolor bioluminescence images of intracranial xenografts bearing HOXD-AS2-overexpressing P-GBM2 or vector control cells in the absence or presence of TMZ on the days as indicated. representative H&E staining for tumor cytostructure. scale bar =2mm. D, IHC analysis of MGMT, γ -H2AX and cleaved caspase-3 expression in intracranial xenografts, scale bar =50 μ m. E, survival curve of HOXD-AS2-overexpressing P-GBM2 or vector control cells-derived intracranial xenografts. F, representative images of tumors originated from D54 HOXD-AS2-overexpressing or vector control cells on the 42nd day. G, growth curve of D54 HOXD-AS2-overexpressing or vector control cells-derived subcutaneous tumor xenografts after treatment with TMZ. H, tumor weight is means of three independent experiments \pm SEM. I, Levels of HOXD-AS2 were analyzed in GBM and NBT of TCGA database. J, Kaplan–Meier curves showing the overall survival of patients with high or low expression of HOXD-AS2 in GBM patients receiving TMZ therapy using the TCGA database. Results are representative of three independent experiments. Student's t-tests were performed. Data are presented as mean \pm SEM (**P<0.01, #P> 0.05).



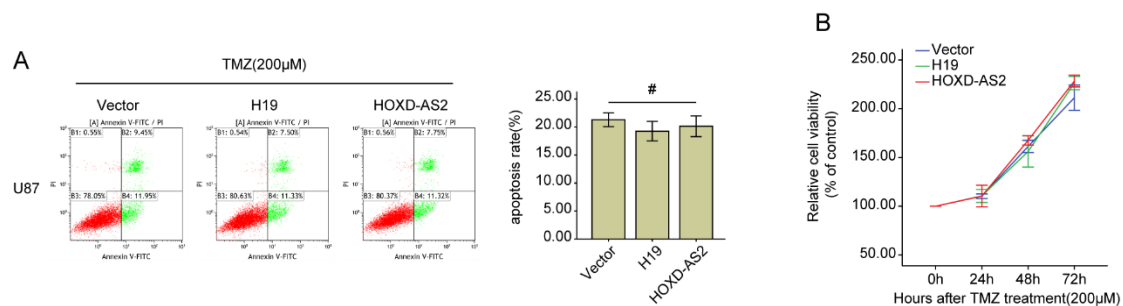
Supplementary Figure 13. H19 overexpression confers TMZ resistance *in vivo*. A, GBM cells transfected with vector, H19-wt or H19-mut were treated with DMSO or 200 μM TMZ at indicated time. Cell proliferation was evaluated using CCK8 assay. B, representative images of tumors originated from D54 cells stably expressing vector, H19-wt or H19-mut on the 42nd day. C, growth curve of D54 cells-derived subcutaneous tumor xenografts after treatment with TMZ. D, tumor weight is means of three independent experiments \pm SEM. One-way ANOVA were performed. Data are presented as mean \pm SEM (**P<0.01).



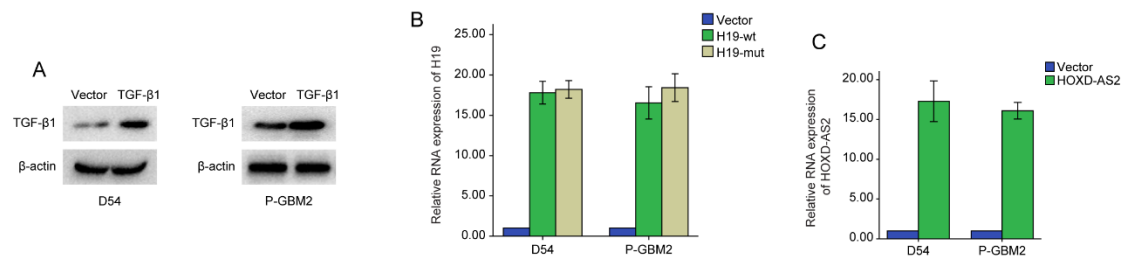
Supplementary Figure 14. TGF-β1, H19 or HOXD-AS2 depletion sensitizes P-GBM2-R cells (P-GBM2 TMZ- resistance cells) to TMZ *in vitro*. A, the levels of TGF-β1, H19 and HOXD-AS2 in P-GBM2-R cells transfected with TGF-β1, H19 or HOXD-AS2-specific siRNA (siTGF-β1, siH19 or siHOXD-AS2) or normal control siRNA (NC). B, P-GBM2-R cells transfected with NC, siTGF-β1, siH19 or siHOXD-AS2 were exposed to 200 μM TMZ for 48 hours and the apoptosis was measured by flowcytometry. C, P-GBM2-R cells transfected with NC, siTGF-β1, siH19 or siHOXD-AS2 were treated with 200 μM TMZ at indicated time. Cell proliferation was evaluated using CCK8 assay. D, Western blot analysis for MGMT, γ-H2AX, H2AX, caspase-3 and cleaved caspase-3. Results are representative of three independent experiments. Student's t-tests were performed. Data are presented as mean ± SEM (**P<0.01).



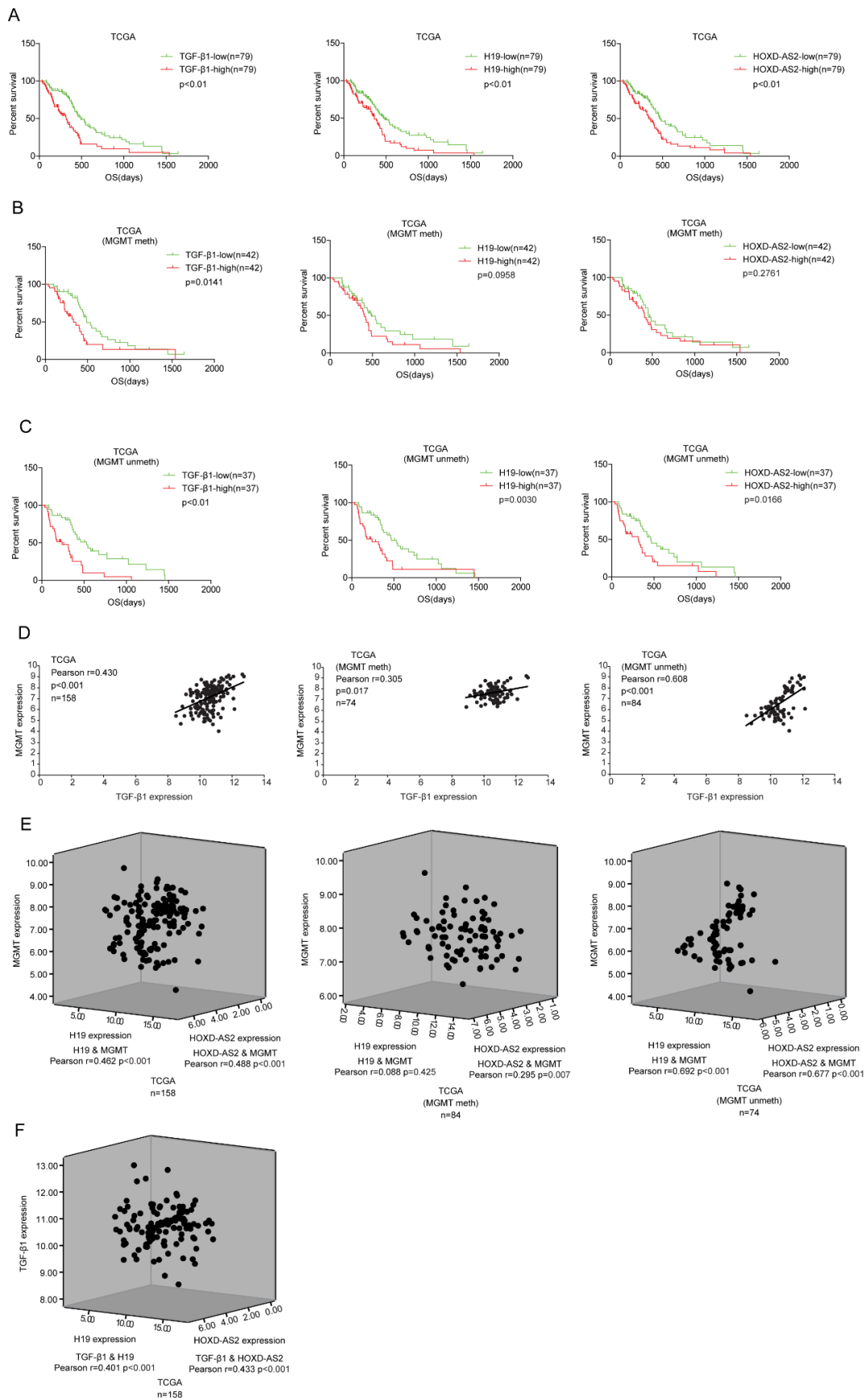
Supplementary Figure 15. The levels of H3K27me3 in the promoter of miR-181a. Expression levels of H3K27me3 in 3 normal brain tissues, 12 GBM tissues and cell lines were analyzed by Chromatin immunoprecipitation. ChIP assays were performed using anti-IgG or specific antibody against Histone H3 (tri methyl K27). The eluted DNA was subjected to qRT-PCR with the specific primer set for miR-181a. Enrichment is presented as the fold change in the level of immunoprecipitated H3K27me3 relative to that of immunoprecipitated IgG (negative control). qRT-PCR results were calculated as $2^{-\Delta\Delta CT}$ (Ct of sample – Ct of input). Graphs show representative experiments.



Supplementary Figure 16. U87 cells transfected with vector, H19 or HOXD-AS2 were exposed to 200μM TMZ for 48 hours and the apoptosis was measured by flowcytometry. Cell proliferation was evaluated using CCK8 assay. Results are representative of three independent experiments. Student's t-tests were performed. Data are presented as mean \pm SEM (# $P > 0.05$).



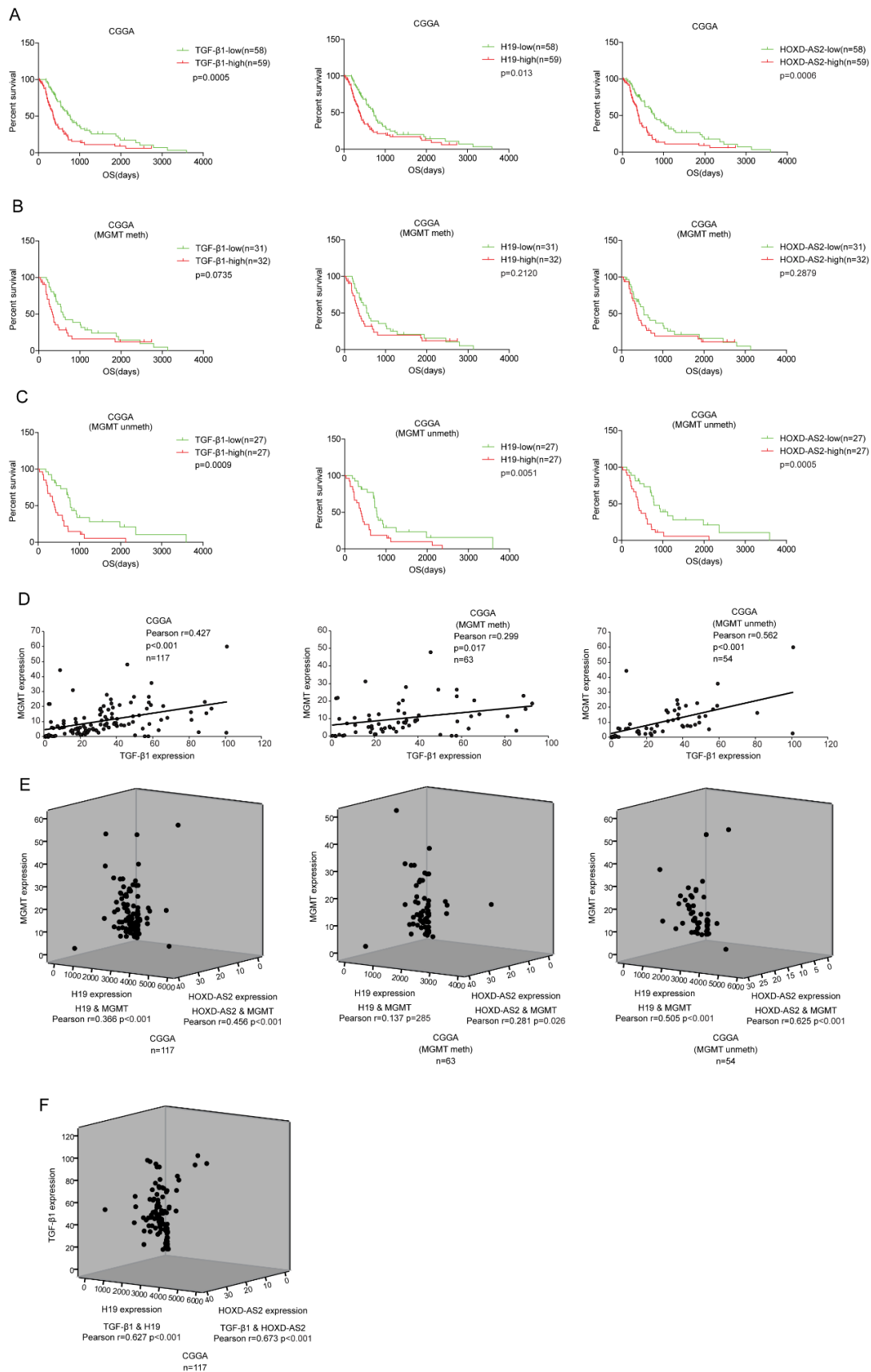
Supplementary Figure 17. A, Western blot analysis of the level of TGF-β1 in GBM cells transfected with vector or TGF-β1 expression plasmid using anti-TGF-β1 antibody. B, qRT-PCR analysis of the level of H19 in GBM cells transfected with vector, H19-wt or H19-mut. C, qRT-PCR analysis of the level of HOXD-AS2 in GBM cells transfected with vector or HOXD-AS2.



303

304 **Supplementary Figure 18.** A, Kaplan Meier survival curves for TGF- β 1, H19 and

HOXD-AS2 expression in GBM of TCGA cohort. B, Kaplan Meier survival curves for
TGF- β 1, H19 and HOXD-AS2 expression in MGMT-meth GBM of TCGA cohort. C,
Kaplan Meier survival curves for TGF- β 1, H19 and HOXD-AS2 expression in MGMT-
unmeth GBM of TCGA cohort. D, The correlation of TGF- β 1 with MGMT in MGMT-
meth or MGMT-unmeth patients. E, the relationship among H19, HOXD-AS2 and
MGMT in MGMT-meth or MGMT-unmeth GBM of TCGA cohort. F, the relationship
among H19, HOXD-AS2 and TGF- β 1 in GBM of TCGA cohort.

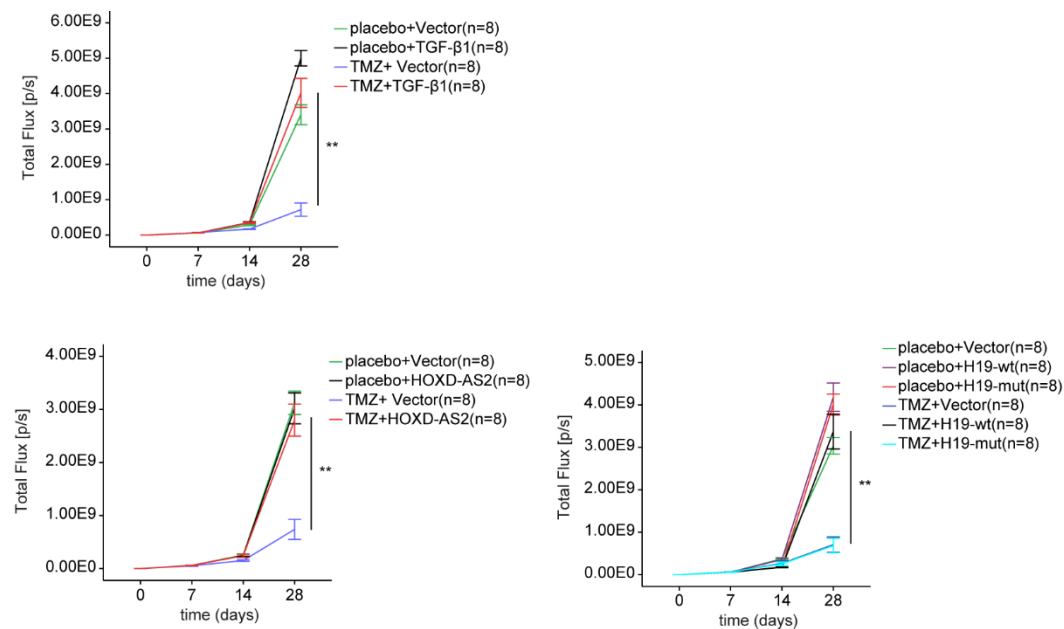


313

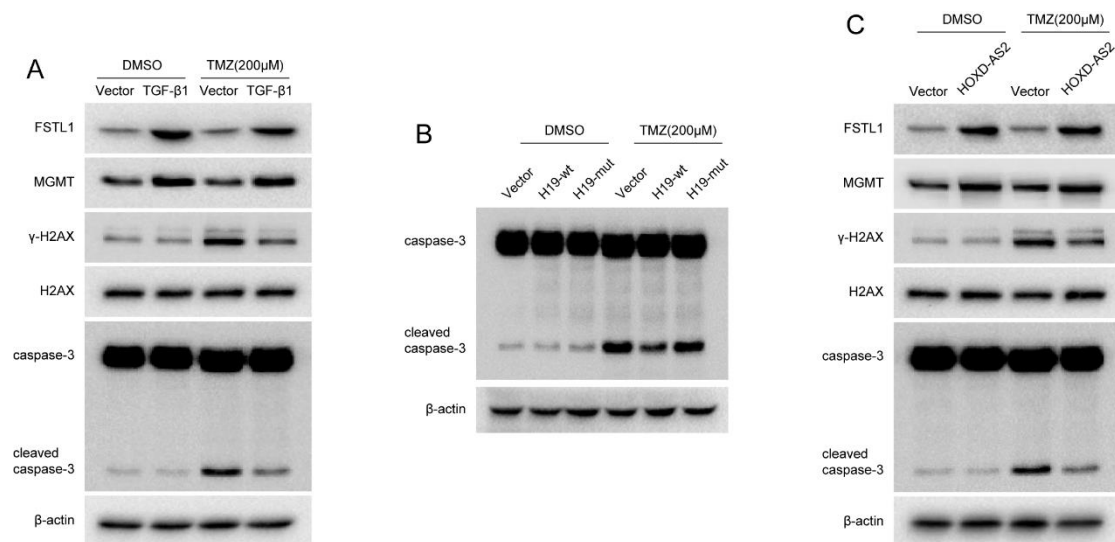
314 **Supplementary Figure 19.** A, Kaplan Meier survival curves for TGF- β 1, H19 and

315 HOXD-AS2 expression in primary GBM of CGGA cohort. B, Kaplan Meier survival

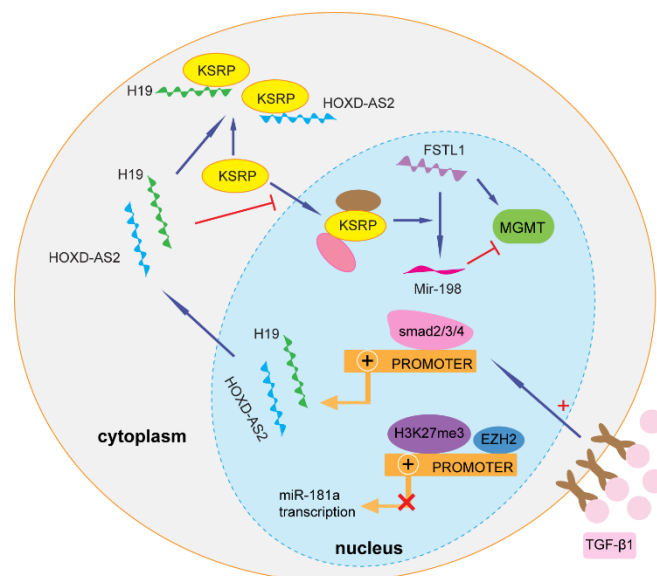
curves for TGF- β 1, H19 and HOXD-AS2 expression in MGMT-meth primary GBM of CGGA cohort. C, Kaplan Meier survival curves for TGF- β 1, H19 and HOXD-AS2 expression in MGMT-unmeth primary GBM of CGGA cohort. D, The correlation of TGF- β 1 with MGMT in MGMT-meth or MGMT-unmeth patients. E, the relationship among H19, HOXD-AS2 and MGMT in MGMT-meth or MGMT-unmeth primary GBM of CGGA cohort. F, the relationship among H19, HOXD-AS2 and TGF- β 1 in primary GBM of CGGA cohort.



Supplementary Figure 20. Growth curve of intracranial xenograft tumors were drawn on bioluminescence images to quantify photon fluxes per second.



Supplementary Figure 21. A, D54 cells infected with lentivirus expressing TGF-β1 or vector control were exposed to DMSO or 200 μM TMZ for 48 hours. Western blot analysis for the indicated proteins. B, D54 cells transfected with vector, H19-wt or H19-mut were treated with DMSO or 200 μM TMZ for 48h. Western blot analysis for cleaved caspase-3. C, D54 cells infected with lentivirus expressing HOXD-AS2 or vector control were exposed to DMSO or 200 μM TMZ for 48 hours. Western blot analysis for the indicated proteins.



Supplementary Figure 22. the diagram summarizes our findings. TGF-β1 binds to type I and II receptors, and promotes Smad2/3 protein phosphorylation. Activated

Smad2/3 proteins associate with Smad4, translocate to the nucleus, and bind to the promoter of H19 and HOXD-AS2 to facilitate transcription. H19 and HOXD-AS2 competitively combine to KSRP and prevent KSRP from participating in FSTL1/miR-198 switching. High levels of H3K27me3 within the miR-181a promoter region prohibit Smad2/3/4 binding to the promoter of miR-181a.

References

1. Louis DN, Ohgaki H, Wiestler OD, et al. The 2007 WHO classification of tumours of the central nervous system. *Acta Neuropathol.* 2007; 114(2):97-109.
2. Liu X, Li Y, Qian Z, et al. A radiomic signature as a non-invasive predictor of progression-free survival in patients with lower-grade gliomas. *NeuroImage. Clinical.* 2018; 20:1070-1077.
3. Wang Y, Qian T, You G, et al. Localizing seizure-susceptible brain regions associated with low-grade gliomas using voxel-based lesion-symptom mapping. *Neuro-oncology.* 2015; 17(2):282-288.
4. Nie E, Jin X, Wu W, et al. BACH1 Promotes Temozolomide Resistance in Glioblastoma through Antagonizing the Function of p53. *Sci Rep.* 2016; 6:39743.
5. Luo H, Chen Z, Wang S, et al. c-Myc-miR-29c-REV3L signalling pathway drives the acquisition of temozolomide resistance in glioblastoma. *Brain : a journal of neurology.* 2015; 138(Pt 12):3654-3672.
6. Matteo B, Federico A, Marianela M, Gian Gaetano T. Predicting protein associations with long noncoding RNAs. *Nature Methods.* 2011; 8(6):444.